Available online at www.sciencedirect.com
ScienceDirect
International Journal of Heat and Mass Transfer 50 (2007) 2874–2882
International Journal of HEAT and MASS TRANSFER
www.elsevier.com/locate/ijhmt

Mixed convection heat transfer in horizontal rectangular ducts with radiation effects

Han-Chieh Chiu [a], Jer-Huan Jang [a], Wei-Mon Yan [b,*]

[a] Department of Mechanical Engineering, Northern Taiwan Institute of Science and Technology, Pei-To, Taipei 112, Taiwan, ROC
[b] Department of Mechatronic Engineering, Huafan University, Shih Ting, Taipei 223, Taiwan, ROC

Received 27 July 2006; received in revised form 6 January 2007
Available online 23 March 2007

Abstract

The study of mixed convection heat transfer in horizontal ducts with radiation effects has been numerically examined in detail. This work is primarily focused on the interaction of the thermal radiation with mixed convection for a gray fluid in rectangular horizontal ducts. The vorticity–velocity method is employed to solve the three-dimensional Navier–Stokes equations and energy equation simultaneously. The integro-differential radiative transfer equation was solved by the discrete ordinates method. The attention of the results is focused on the effects of thermal buoyancy and radiative transfer on the development of temperature, the friction factor and the Nusselt number. Results reveal that radiation effects have a considerable impact on the heat transfer and would reduce the thermal buoyancy effects. Besides, the development of temperature is accelerated by the radiation effects.

Keywords: Mixed convection; Horizontal rectangular ducts; Radiation effects

1. Introduction

Thermal radiation with combined buoyancy and forced convection is encountered in a wide range of the thermal engineering applications, such as heat exchangers, thermal insulation, and cooling processes in nuclear reactors. Separate calculation of radiation and convection effects and superposition without considering their interaction leads to significant errors as radiation and convection effects are similarly important. In such cases, the momentum, energy and radiation transport equations should be solved simultaneously to determine the velocity and temperature fields and heat transfer rate accurately.

Massive amount of works, both theoretical and experimental, have been done on mixed convection heat transfer in internal laminar or turbulent flows [1–8]. Cheng et al. [9], Ou et al. [10] and Cheng and Ou [11] employed the assumption of large Prandtl number to study the mixed convection heat transfer in the thermal entrance region of horizontal rectangular channels. The same problems were also examined for a horizontal tube by Hieber and Sreenivasan [12], Hong et al. [13], Ou and Cheng [14] and Hishida et al. [15]. Their results showed that the secondary flow induced by the thermal buoyancy force can enhance significantly the heat transfer. In addition, the buoyancy would decrease the thermal entrance length. However, heat transfer by mixed convection and radiation has not been studied extensively. Forced convection in a channel with radiation has been under investigation by many researchers [16–19] for ducts with prescribed heat fluxes and temperature distributions on wall surface. These studies used various approximate methods for radiative transport in the medium. Among these, the differential approximation methods describe approximation variation of the intensity of radiation as a function of position and angle.

In recent years, heat transfer by simultaneous free or mixed convection and radiation has drawn the attention of the researchers [20–24] due to its importance in combustion, furnace design, fluidized-bed heat exchangers, and the

* Corresponding author. Tel.: +886 2 2663 2102; fax: +886 2 2663 1119.
E-mail address: wmyan@huafan.hfu.edu.tw (W.-M. Yan).

0017-9310/$ - see front matter © 2007 Elsevier Ltd. All rights reserved.
doi:10.1016/j.ijheatmasstransfer.2007.01.010

Nomenclature

A	cross-sectional area of horizontal rectangular ducts (m^2)
a, b	height and width of horizontal rectangular ducts, respectively (m)
c_p	specific heat ($J\,kg^{-1}\,K^{-1}$)
De	equivalent hydraulic diameter, $2ab/(a+b)$
f	friction factor, $2\tau_w/(\rho_o w_o^2)$
g	acceleration due to gravity, m/s^2
G, G^*	dimensional and dimensionless incident radiation, $G^* = \frac{G}{(4\vec{n}^2\sigma T_w^4)}$
Gr	Grashof number, $g\beta\,(T_w - T_o)De^3/\nu^2$
$\bar{h}$	circumferentially average heat transfer coefficient ($W\,m^{-2}\,K^{-1}$)
k	thermal conductivity ($W\,m^{-1}\,K^{-1}$)
m, m'	direction of the discrete ordinates
M, N	number of the finite difference divisions in X- and Y-directions, respectively
n	direction coordinate normal to the duct wall
$\bar{n}$	refractive index
N^*	order of phase function
N_c	conduction-to-radiation parameter, $k\kappa/(4\vec{n}^2\sigma T_w^4)$
Nu_c	local convective Nusselt number
Nu_r	local radiative Nusselt number
Nu_t	local total Nusselt number
$\bar{p}$	cross-sectional mean pressure (kPa)
$\overline{P}$	dimensionless cross-sectional mean pressure
p'	perturbation term about mean pressure (kPa)
P'	dimensionless perturbation pressure
Pe	Peclet number, $Pr \cdot Re$
P_n	Legendre polynomial
Pr	Prandtl number, ν/α
Q_r	dimensionless radiation flux
$\vec{q}_c$	convective heat flux ($W\,m^{-2}$)
$\vec{q}_r$	radiative heat flux ($W\,m^{-2}$)
$\vec{q}_t$	total heat flux ($W\,m^{-2}$)
Ra	Rayleigh number, $Pr \cdot Gr$
Re	Reynolds number, $w_o D_e/\nu$
T	temperature (K)
T_o	inlet temperature (K)
U, V, W	dimensionless velocity components in the X-, Y-, Z-directions, respectively
u, v, w	velocity components in the x-, y-, z-directions, respectively ($m\,s^{-1}$)
w_o	uniform velocity at the inlet, m/s
X, Y, Z	dimensionless rectangular coordinate, $X = x/D_e$, $Y = y/D_e$, $Z = z/(D_e \cdot Re)$
Z^*	dimensionless z-direction coordinate, $z/(Pr \cdot Re \cdot D_e) = Z/Pr$
x, y, z	rectangular coordinate system (m)

Greek symbols

α	thermal diffusivity ($m^2\,s^{-1}$)
β	coefficient of thermal expansion (K^{-1})
$\bar{\beta}$	extinction coefficient, m^{-1}
$\vec{I}, \vec{I}'$	outward and inward direction of radiation
ε_w	wall emissivity
γ	aspect ratio of a rectangular duct, b/a
κ_s	scattering coefficient, m^{-1}
μ, η, ζ	direction cosines
θ	dimensionless temperature, T/T_w
θ^o	dimensionless inlet temperature, T_o/T_w
ν	kinematic viscosity ($m^2\,s^{-1}$)
ϕ	scattering phase function
ρ	density ($kg\,m^{-3}$)
σ	Stefan–Boltzmann constant, $5.67 \times 10^{-8}\,W/m^2\,K^{-4}$
τ	optical thickness
τ_w	wall shear stress, kPa
ω	single scattering albedo
ξ	dimensionless vorticity in the axial direction, $\partial U/\partial Y - \partial V/\partial X$
ψ	dimensionless radiation intensity, $\pi I/(\vec{n}^2\sigma T_w^4)$
Ω	solid angle

Superscript

$\bar{}$	mean quantity

Subscripts

b	bulk fluid quantity
c	convective
o	condition at inlet
r	radiative
w	value at wall

design of high temperature gas-cooled nuclear reactors. Bakier and Gorla [25] have investigated the effect of radiation on the mixed convection flow over a cylinder embedded in a porous medium. Bakier [26] reported the effect of the radiation on the mixed convection flow on an isothermal vertical surface in a saturated porous medium and obtained a similarity solution. Later, Kim and Fedorov [27] studied the viscous incompressible micropolar fluid flow past a semi-infinite vertical porous plate with the presence of thermal radiation field. However, these studies are limited to porous medium. Recently, Sediki et al. [28] investigated the interaction between radiation and mixed convection for ascending flows in vertical tubes. They found that the radiation tends to reduce the velocity distortion effect of buoyancy for heated gases.

Knowing from the paper review cited above, no numerical study has been published of simultaneous effect of mixed convection and radiation in horizontal rectangular duct

flows. This motivates present study. Besides, the flow is considered to be hydrodynamically and thermally developing.

2. Analysis

In this study of thermal radiation effect, flow is assumed to be laminar for simplicity although the flow is practically turbulent. Consider a steady three-dimensional laminar flow of gas in the entrance region of a horizontal rectangular duct, as schematically shown in Fig. 1. Gravity is set along the negative direction of y-axis. The height and width of the rectangular ducts are set to be a and b, respectively. The walls are imposed uniform and constant temperature, T_w. The u, v and w are the velocity components in the x-, y- and z-directions, respectively. The flow entering the duct has a uniform axial velocity w_o and temperature T_o. In order to simplify the calculation, the fluid properties are taken to be constant except the density in the buoyancy term of the momentum equation. The Boussinesq approximation is employed for the thermal buoyancy effect. Various energy dissipations and compression effects in the energy equation are neglected due to the laminar flow. In addition, the fluid is considered as gray, absorbing, emitting, and scattering.

The flow is considered to be parabolic for this study. In the momentum equations, a space-averaged pressure $\bar{p}$ is imposed to prevail at each cross-section, permitting a decoupling of the pressure in the cross-sectional momentum equation. Together with the neglect of axial diffusion of momentum and heat, the dynamic pressure p_m can then be presented as the sum of a cross-sectional mean pressure, $\bar{p}(z)$, which drives the main flow, and a perturbed pressure about the mean, $p'(x,y,z)$, which drives the cross-stream flow,

$$p_m = \bar{p}(z) + p'(x,y,z) \tag{1}$$

For systematical analysis, the dimensionless groups are introduced as follows:

$$\begin{aligned}
&X = x/De;\quad Y = y/De;\quad Z = z/(De\cdot Re);\quad Z^* = Z/Pr;\quad U = uDe/v;\\
&V = vDe/v;\quad W = w/w_o;\quad \theta_0 = T_o/T_w;\quad \theta = T/T_w;\quad \overline{P} = \bar{p}/(\rho_o w_o^2)\\
&P' = p'/(\rho_o v^2/De^2);\quad Pr = v/\alpha;\quad Re = w_o De/v\\
&Gr = g\beta(T_w - T_o)De^3/v^2;\quad Ra = Pr\cdot Gr;\\
&\gamma = b/a;\quad N_c = k\kappa/(4\bar{n}^2\sigma T_w^3)\\
&G^* = G/(\bar{n}^2\sigma T_w^4);\quad \tau = \kappa De;\quad \omega = \kappa_s/\kappa
\end{aligned} \tag{2}$$

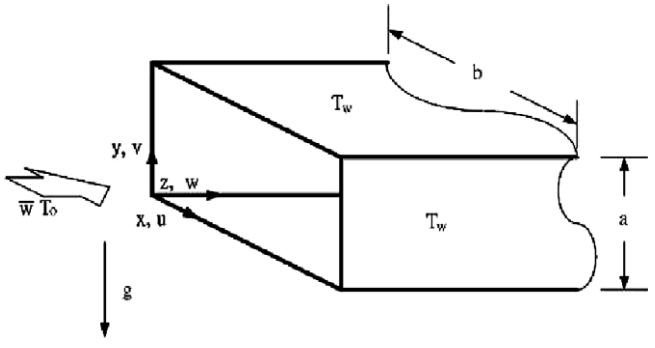

Fig. 1. Schematic diagram of the physical system.

The governing equations are those for conservation of mass, momentum, and energy. The non-dimensional governing equations can be formulated as follows:

Continuity equation

$$\frac{\partial U}{\partial X} + \frac{\partial V}{\partial Y} + \frac{\partial W}{\partial Z} = 0 \tag{3}$$

Momentum equations

$$U\frac{\partial U}{\partial X} + V\frac{\partial U}{\partial Y} + W\frac{\partial U}{\partial Z} = -\frac{\partial P'}{\partial X} + \frac{\partial^2 U}{\partial X^2} + \frac{\partial^2 U}{\partial Y^2} \tag{4}$$

$$U\frac{\partial V}{\partial X} + V\frac{\partial V}{\partial Y} + W\frac{\partial V}{\partial Z} = -\frac{\partial P'}{\partial X} + \frac{\partial^2 V}{\partial X^2} + \frac{\partial^2 V}{\partial Y^2} + \frac{Ra}{Pr}\cdot\frac{\theta - \theta_o}{1-\theta_o} \tag{5}$$

$$U\frac{\partial W}{\partial X} + V\frac{\partial W}{\partial Y} + W\frac{\partial W}{\partial Z} = -\frac{\partial \overline{P}}{\partial Z} + \frac{\partial^2 W}{\partial X^2} + \frac{\partial^2 W}{\partial Y^2} \tag{6}$$

Energy equation

$$U\frac{\partial \theta}{\partial X} + V\frac{\partial \theta}{\partial Y} + W\frac{\partial \theta}{\partial Z} = \frac{1}{Pr}\left[\frac{\partial^2\theta}{\partial X^2} + \frac{\partial^2\theta}{\partial Y^2} + \frac{(1-\omega)\tau^2}{N_c}\cdot(G^* - \theta^4)\right] \tag{7}$$

The non-dimensional axial vorticity can be expressed as

$$\xi = \partial U/\partial Y - \partial V/\partial X \tag{8}$$

The axial vorticity transport equation and the continuity equation can then be derived or reformulated as follows:

$$\begin{aligned}
&U\frac{\partial \xi}{\partial X} + V\frac{\partial \xi}{\partial Y} + W\frac{\partial \xi}{\partial Z} + \xi\left(\frac{\partial U}{\partial X} + \frac{\partial V}{\partial Y}\right)\\
&\quad + \left(\frac{\partial W}{\partial Y}\cdot\frac{\partial U}{\partial Z} - \frac{\partial W}{\partial X}\cdot\frac{\partial V}{\partial Z}\right)\\
&\quad = \frac{\partial^2\xi}{\partial X^2} + \frac{\partial^2\xi}{\partial Y^2} - \frac{Ra}{Pr}\cdot\frac{\partial\theta/\partial X}{1-\theta_o}
\end{aligned} \tag{9}$$

$$\frac{\partial^2 U}{\partial X^2} + \frac{\partial^2 U}{\partial Y^2} = \frac{\partial \xi}{\partial Y} - \frac{\partial^2 W}{\partial X \partial Z} \tag{10}$$

$$\frac{\partial^2 V}{\partial X^2} + \frac{\partial^2 V}{\partial Y^2} = -\frac{\partial \xi}{\partial X} - \frac{\partial^2 W}{\partial Y \partial Z} \tag{11}$$

Along the duct, the conservation of mass requires that the mass flow rate at any axial location be the same, hence

$$\int_0^{\frac{1+\gamma}{2\gamma}}\int_0^{\frac{1+\gamma}{2}} W\,\mathrm{d}X\,\mathrm{d}Y = \frac{(1+\gamma)^2}{4\gamma} \tag{12}$$

This relation is employed to deduce the pressure gradient in the axial momentum equation.

Concerning the radiation in the problem, the medium is considered as gray, absorbing and scattering. The dimensionless form of the radiation transfer equation is expressed as

$$\mu\frac{\partial \psi}{\partial X} + \eta\frac{\partial \psi}{\partial Y} + \tau\psi = (1-\omega)\tau\theta^4 + \frac{\omega\tau}{4\pi}\int_{\Gamma'=4\pi}\phi(\vec{\Gamma}', \vec{\Gamma})\psi\,\mathrm{d}\Gamma' \tag{13}$$

where ψ is the dimensionless intensity of radiation at a location of (X, Y), which is of the form $\pi I/(\vec{n}^2\sigma T_w^4)$. In the equation, the axial term, $\frac{\partial\psi}{\partial Z}$, is dropped by assuming $\frac{\partial q_{rz}}{\partial Z} \ll \frac{\partial q_{rx}}{\partial X} + \frac{\partial q_{ry}}{\partial Y}$. The parameters μ, η, and ζ are the direction cosines for the radiation direction $\vec{\Gamma}$. The symbol ϕ is the scattering phase function, which can be expressed in terms of Legendre polynomials as

$$\phi(\vec{\Gamma}', \vec{\Gamma}) = \sum_{n=0}^{N} a_n P_n(\mu'\mu + \eta'\eta + \xi'\xi) \tag{14}$$

For a gray, opaque, diffusively emitting, and reflecting surface, the boundary condition is

$$\psi_w(\vec{\Gamma}) = \varepsilon_w + \frac{1-\varepsilon_w}{\pi} \int_{\vec{n}\cdot\vec{\Gamma}'<0} |\vec{n}\cdot\vec{\Gamma}'|\psi_w(\vec{\Gamma}')\,d\Gamma', \quad \vec{n}\cdot\vec{\Gamma} > 0 \tag{15}$$

where ε_w is the wall emissivity, and $\vec{n}$ is the unit normal vector pointing away from the duct wall into the medium.

Once the dimensionless radiation intensity ψ is known, the dimensionless radiation flux vector and incident radiation are re-determined from their definitions as

$$\vec{Q}_r = \frac{\vec{q}_r}{(4\bar{n}^2\sigma T_w^4)} = \frac{1}{4\pi}\int_{\Gamma=4\pi} \vec{\Gamma}\psi\,d\Gamma \tag{16}$$

$$G^* = \frac{G}{(4\bar{n}^2\sigma T_w^4)} = \frac{1}{4\pi}\int_{\Gamma=4\pi} \psi\,d\Gamma \tag{17}$$

The corresponding boundary conditions for this study are *Entrance* $(Z = 0)$:

$$W = 1; \quad U = V = \xi = 0; \quad \theta = \theta_o \tag{18}$$

Duct walls:

$$U = V = W = 0; \quad \theta = 1 \tag{19}$$

After obtaining the developing velocity and temperature fields along the axial direction of the rectangular duct, the local friction factor and Nusselt numbers are major parameters of practical interest for the study of mixed convection heat transfer. Following the usual definitions, the expression for the product of the peripherally averaged friction factor and Reynolds number can be expressed as

$$f\,Re = -2\overline{\left.\frac{\partial W}{\partial n}\right|}_{wall} \tag{20}$$

where the overbar represents the average around the perimeters.

Energy transport from the duct wall to the gas flow depends on two related factors – the fluid temperature gradient on the wall and the rate of radiative heat exchange. Therefore, the local total Nusselt number along the duct wall is defined as

$$Nu_t = \frac{\bar{h}D_e}{k} = \frac{q_t D_e}{k(T_w - T_b)} \tag{21}$$

where $q_t = q_c + q_r = -k\partial T/\partial n + q_r$. The function Nu_t is the sum of local convective Nusselt number, Nu_c, and local radiative Nusselt number, Nu_r. They are, respectively, defined as

$$Nu_c = -\frac{\overline{\partial\theta}}{\partial n}\frac{1}{1-\theta_b} \tag{22}$$

and

$$Nu_r = \frac{\tau\overline{Q}_r}{N_c}\frac{1}{1-\theta_b} \tag{23}$$

In the equations, the bulk fluid temperature θ_b is defined as

$$\theta_b = \frac{\int_0^{\frac{1+\gamma}{2\gamma}}\int_0^{\frac{1+\gamma}{2}} \theta\cdot W\,dX\,dY}{\int_0^{\frac{1+\gamma}{2\gamma}}\int_0^{\frac{1+\gamma}{2}} W\,dX\,dY} \tag{24}$$

3. Solution method

In this work, the equations for the unknown U, V, W, ξ, θ and $d\overline{P}/dZ$ are coupled, and the vorticity–velocity method for three-dimensional parabolic flow [29] is employed to solve the governing equations. The field solutions for a given combination of parameters are calculated by a marching technique based on the DuFort–Frankel scheme [30]. The detailed numerical method and solution procedure are available in Ref. [31] and are not presented here. In the present study, the radiative transfer equation is obtained by the discrete ordinates method with S_N quadrature [32–34]. The solid angle 4π is discretized into a finite number of directions, the discrete ordinate forms of radiative transfer equation is applied at these directions with the integral term replaced by a numerical qadrature and becomes

$$\mu_m\frac{\partial\psi_m}{\partial X} + \eta_m\frac{\partial\psi_m}{\partial Y} + \tau\psi_m = (1-\omega)\tau\theta^4 + \frac{\omega\tau}{4\pi}\sum_{m'} w_{m'}^*\phi_{m'm}\psi_m \tag{25}$$

with associated boundary conditions

$$\psi_m = \varepsilon_w + \frac{1-\varepsilon_w}{\pi}\sum_{m'}\psi_{m'}|\mu_{m'}|w_{m'}^*, \quad \mu_m > 0,\ \mu_{m'} < 0,\ X = 0 \tag{26}$$

$$\psi_m = \varepsilon_w + \frac{1-\varepsilon_w}{\pi}\sum_{m'}\psi_{m'}|\mu_{m'}|w_{m'}^*, \quad \mu_m < 0,\ \mu_{m'} > 0,\ X = \frac{1+\gamma}{2} \tag{27}$$

$$\psi_m = \varepsilon_w + \frac{1-\varepsilon_w}{\pi}\sum_{m'}\psi_{m'}|\eta_{m'}|w_{m'}^*, \quad \eta_m > 0,\ \eta_{m'} < 0,\ Y = 0 \tag{28}$$

$$\psi_m = \varepsilon_w + \frac{1-\varepsilon_w}{\pi}\sum_{m'}\psi_{m'}|\eta_{m'}|w_{m'}^*, \quad \eta_m < 0,\ \eta_{m'} > 0,\ Y = \frac{1+\gamma}{2\gamma} \tag{29}$$

where subscript m and m' represent the direction of the discrete ordinates and w_m^* are the quadrature weights.

The discrete form of the phase function $\phi_{m'm}$ is expressed as

$$\phi_{m'm} = \sum_{n=0}^{N^*} a_n P_n(\mu_{m'}\mu_m + \eta_{m'}\eta_m + \zeta_{m'}\zeta_m) \tag{30}$$

Table 1
The discrete directions and quadrature weights for the S_6 method (one octant only)

m	μ_m	η_m	ζ_m	w_m^*
1	0.948235	0.224556	0.224556	$\pi/6$
2	0.689048	0.689048	0.224556	$\pi/6$
3	0.224556	0.948235	0.224556	$\pi/6$
4	0.689048	0.224556	0.689048	$\pi/6$
5	0.224556	0.689048	0.689048	$\pi/6$
6	0.224556	0.224556	0.948235	$\pi/6$

Table 2
Effects of grid size on local Nu_t for $Ra = 5 \times 10^4$, $N_c = 0.1$, $\tau = 1$, $\omega = 0$ and $\varepsilon_w = 0.5$

$M \times N(\Delta Z^*)$	Z^*					
	0.001	0.005	0.01	0.05	0.1	0.3
$51 \times 51(1 \times 10^{-5}$–$2 \times 10^{-4})$	13.69	7.52	6.62	7.60	6.87	5.87
$81 \times 81(1 \times 10^{-5}$–$2 \times 10^{-4})$	13.40	7.50	6.60	7.56	6.86	5.86
$51 \times 51(1 \times 10^{-6}$–$2 \times 10^{-4})$	13.85	7.54	6.63	7.60	6.87	5.87
$31 \times 31(1 \times 10^{-5}$–$2 \times 10^{-4})$	15.33	7.60	6.68	7.66	6.87	5.86

The integro-differential radiative transfer equation is transformed by the angular discretization into a set of coupled partial differential equations. Therefore, the accuracy of the S_N method is dependent on the choice of the quadrature scheme. S_6 scheme is employed for present study, so the total number of the discrete direction is 24. The momentum-marching technique [35] is used to calculate the discrete directions and quadrature weights listed in Table 1. The dimensionless radiation intensity, radiation flux, and incident radiation are calculated by solving Eqs. (25)–(30) using procedure described by Modest [34].

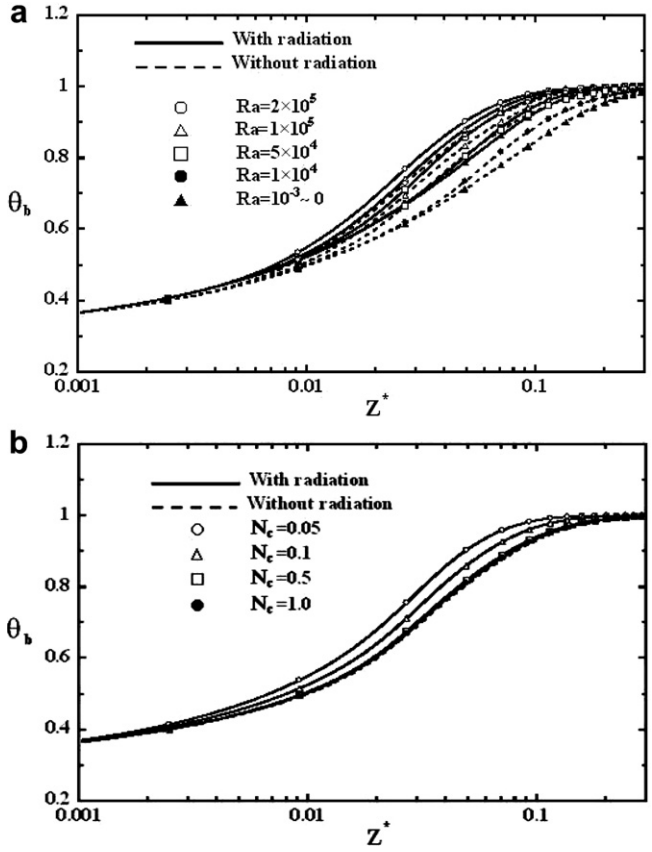

Fig. 2. Effect of (a) Rayleigh number and (b) conduction-to-radiation parameter on the bulk temperature distribution along the axial direction.

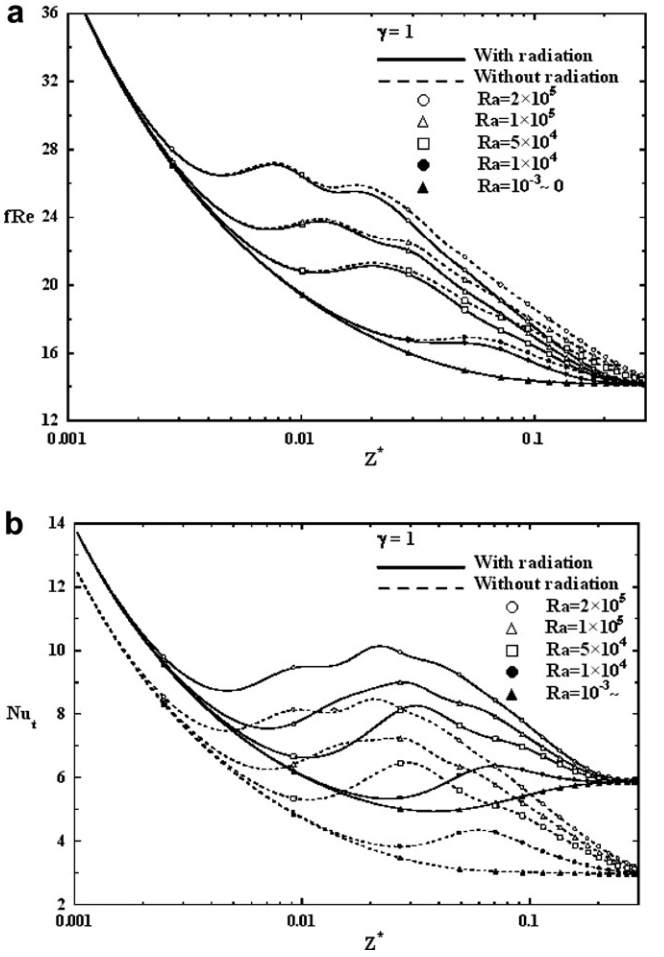

Fig. 3. Effect of Rayleigh number on the local (a) friction factor and (b) Nusselt number for $\gamma = 1$.

The grid distributions were arranged to be uniform in the cross-sectional plane but non-uniformly in the axial direction for the uneven variations of the field properties in the entrance region. In order to check the independence of the grid points of the numerical results, a numerical experiment was carried out with various grid distributions in the cross-sectional plane ($M \times N$) and axial step size (ΔZ^*). There are four grid distribution tested in the analysis and shown in Table 2, and they are $31 \times 31(1 \times 10^{-5}$–$2 \times 10^{-4})$, $51 \times 51(1 \times 10^{-5}$–$2 \times 10^{-4})$, $51 \times 51(1. \times 10^{-6}$–$2 \times 10^{-4})$, and $81 \times 81(1 \times 10^{-5}$–$2 \times 10^{-4})$. For $Ra = 5 \times 10^4$, $N_c = 0.1$, $\tau = 1, \omega = 0$ and $\varepsilon_w = 0.5$, it is found from Table 2 that the deviations in local total Nusselt number Nu_t calculated with $51 \times 51(1 \times 10^{-5}$–$2 \times 10^{-4})$ and $81 \times 81(1 \times 10^{-5}$–$2 \times 10^{-4})$ are always less than 2%. Furthermore, the deviations in Nu_t calculated with $51 \times 51(1 \times 10^{-5}$–$2 \times 10^{-4})$ and $51 \times 51(1 \times 10^{-6}$–$2 \times 10^{-4})$

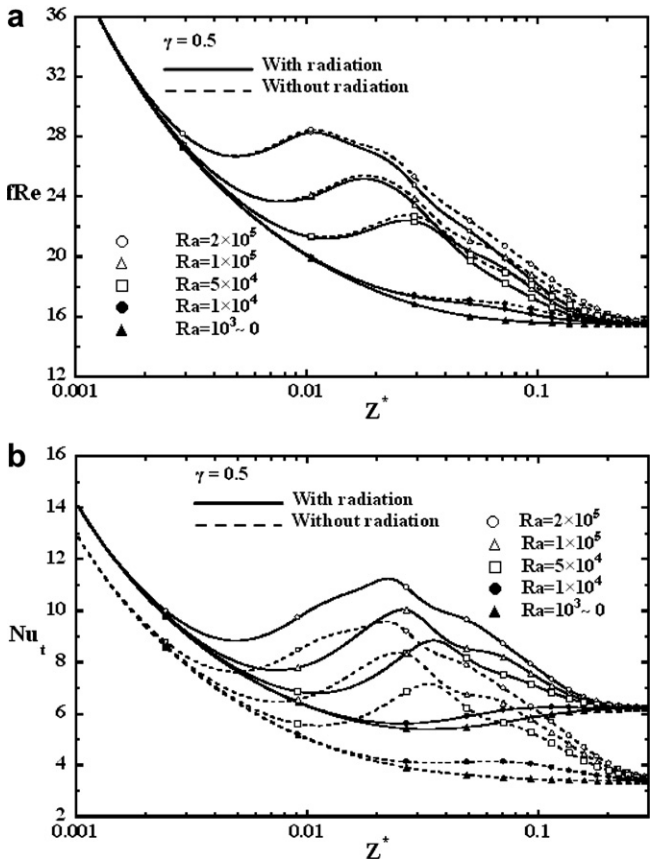

Fig. 4. Effect of Rayleigh number on the local (a) friction factor and (b) Nusselt number for $\gamma = 0.5$.

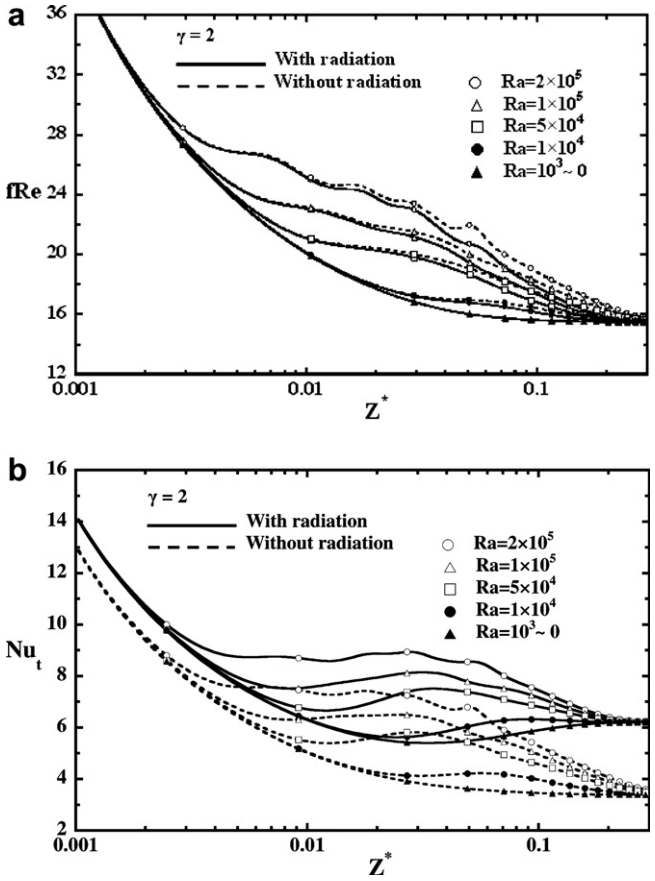

Fig. 5. Effect of Rayleigh number on the local (a) friction factor and (b) Nusselt number for $\gamma = 2$.

are also less than 2%. Therefore, the computations with grid distribution of $51 \times 51(1 \times 10^{-5}$–$2 \times 10^{-4})$ are considered to be sufficiently accurate to describe the flow and heat transfer in a horizontal rectangular duct. As a partial verification of the computational procedure, results were initially obtained for convection heat transfer in a horizontal rectangular duct without thermal radiation effect and compared with those of Chou and Hwang [8]. The Nusselt number and friction factor were found to agree within 2%. The above program tests indicate that the adopted solution methods are suitable for the present study.

4. Results and discussion

In this work, the results are presented for air flowing in a heated rectangular duct over a certain range of governing parameters. The ratio of air inlet temperature and wall temperature is fixed to be $\theta_o = 0.3$, and the Prandtl number is set to be $Pr = 0.7$. The parameters utilized in this analysis include Rayleigh number, Ra, conduction-to-radiation parameter, N_c, aspect ratio, γ, optical thickness, τ, wall emissivity, ε_w, and single scattering albedo, ω. The Rayleigh number is varied from 1×10^3 to 2×10^5; and the values of conduction-to-radiation parameter are 0.05, 0.1, 0.5 and 1.0. In order to study the geometry effect, the aspect ratio is set to be 0.5, 1, and 2. The optical thickness τ is varied from 0.1 to 2.0, the wall emissivity ε_w is varied from 0.25 to 1.0, and the single scattering albedo ω is varied from 0.0 to 1.0. Numerical solutions were obtained for axial distributions of the bulk temperature, local friction factor, and Nusselt number.

For practical applications, the bulk temperature of the fluid along the channel is important. Fig. 2 presents the effects of Rayleigh number Ra and conduction-to-radiation parameter N_c on the distributions of the bulk temperature. Results without radiation effect, shown as dashed line in Fig. 2, are also sketched for comparison. Results reveal that the effect of radiation on the thermal development is insignificant near the entrance. However, radiation effect tends to equalize the temperature in the flow at the downstream. It is clearly seen that the bulk temperature development is enhanced with larger Ra and smaller N_c. Also, the bulk temperature is the almost the same as that without radiation when N_c is large ($N_c > 0.5$), which corresponds to a weak radiation-convection interaction. It can be easily realized that the bulk temperature is higher with stronger radiation effect ($N_c = 0.05$) due to radiative heat flux being an additional mode of energy transport.

Effects of the channel geometry on the friction factor and Nusselt number are of practical interest. Figs. 3–5 present the effects of Rayleigh number Ra on the distributions of

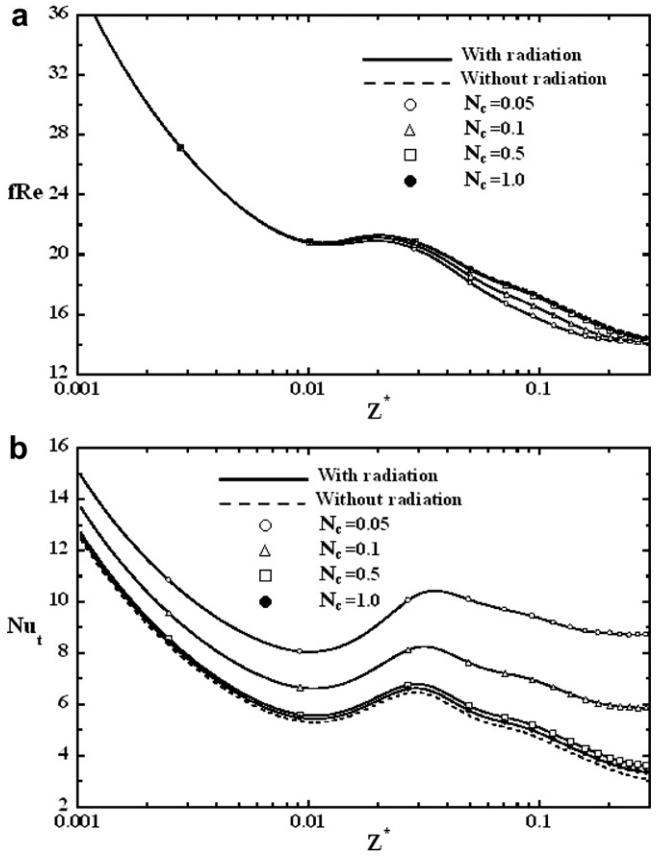

Fig. 6. Effect of conduction-to-radiation parameter on the local (a) friction factor and (b) Nusselt number.

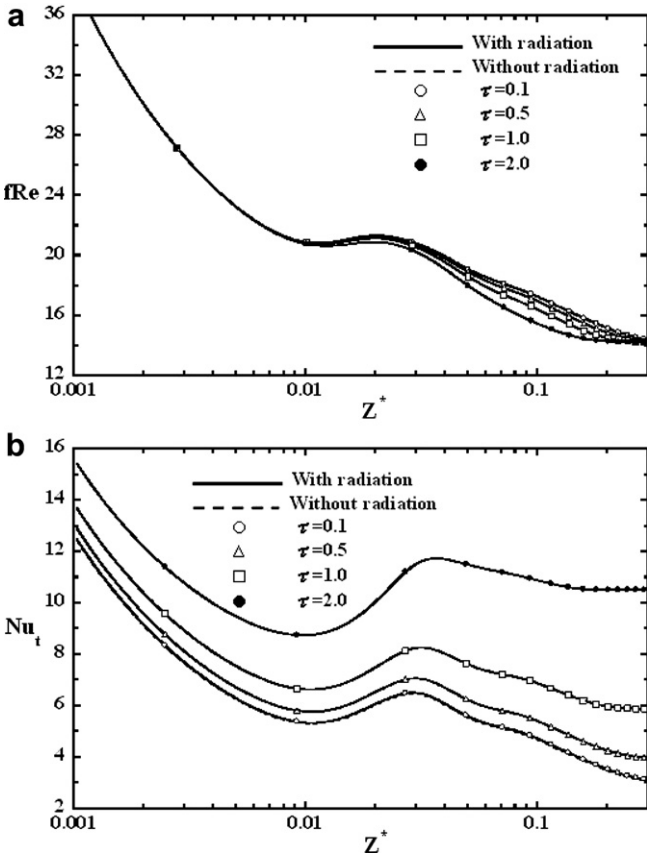

Fig. 7. Effect of optical thickness on the local (a) friction factor and (b) Nusselt number.

the friction factor and the Nusselt number for $\gamma = 1.0$, 0.5, and 2.0, respectively. Results indicate that friction factor with radiation effect is lower than that without radiation effect for three aspect ratio cases. The distributions of Nu_t with low Ra are similar to those of forced convection flow. In other words, Nu_t decreases in the inlet region and then reaches a constant fully-developed value. It is apparent that the buoyancy effects on both fRe and Nu_t are insignificant up to a certain distance, but have a substantial augmentation in further downstream. An overall comparison of Figs. 3–5 reveals that the trend of these curves is similar. But, a close comparison shows that the distributions of the fRe and Nu_t are larger for a ducts with smaller γ. This is due to fact that a duct with smaller γ gives rise to a stronger buoyancy effects than a duct with larger γ does. It is also observed that the fRe and Nu_t at the downstream are the least for $\gamma = 1$ among the three cases. Obviously, effects of Ra are practically negligible as Ra is small ($Ra < 10^4$). It should be noted that fRe and Nu_t increase as Ra increases. The monotonic decreases of fRe and Nu_t near the inlet are due to entrance effect. The onset of buoyancy effect takes place at some axial location from the inlet, depending on the value of Ra.

Fig. 6 shows the effects of the conduction-to-radiation parameter N_c on the axial variation of the local friction factor and Nusselt number. It is clear in Fig. 6a that the fRe is not apparently influenced by N_c in the entrance region, because the convection effect is predominant at the positions. However, the radiation effect becomes more important in the downstream range. It is found that the fRe decreases with a decrease in N_c. This means that friction factor is reduced as radiation effect increases. This may be explained by the fact that the temperature field is flattened with the presence of radiation causing a reduction of buoyancy effect, which in turns leads to the reduction in fRe at the downstream. It is seen in Fig. 6b that the local total Nusselt number Nu_t with radiation is larger than that without radiation. This can be easily understood by the fact that radiation effect is an additional mechanism of heat transfer and the radiation source term in the energy equation augments the rate of thermal development as mentioned above. Therefore, the radiation effect enhances both the heat flux through fluid and the rate of thermal development. It is also noted that the Nu_t converges to the case of no radiation with increasing N_c (> 0.5), suggesting that effect of radiation is negligible as the N_c is larger than 1.0.

Another important factor of radiation properties that affects the heat transfer and fluid flow is the optical thickness τ of the medium. A small τ indicates medium does not absorb and emit much energy, while a large τ means a strongly radiative participating medium. The influence of optical thickness τ on the axial distribution of fRe and

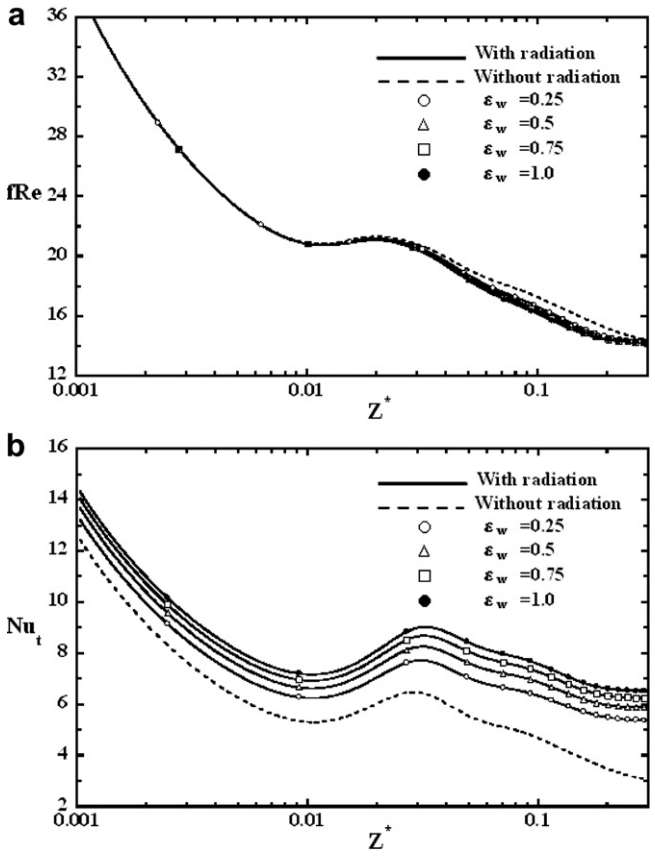

Fig. 8. Effect of wall emissivity on the local (a) friction factor and (b) Nusselt number.

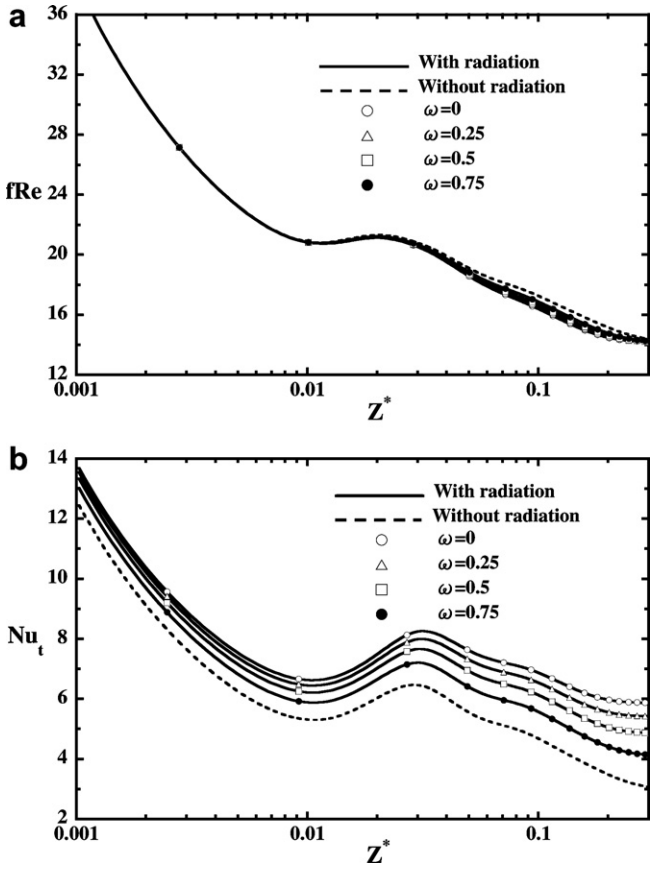

Fig. 9. Effect of single scattering albedo on the local (a) friction factor and (b) Nusselt number.

Nu_t is depicted in Fig. 7. It is clearly seen that the optical thickness does not affect the local fRe till downstream region. The trend of curves is similar to that of Fig. 6a. It is also found that fRe decreases as τ increases at the downstream. A larger τ indicates a stronger radiation effect. That is, the fRe decreases as radiation effect increases. The reason is the same as that mentioned above. It is also shown from Fig. 7b that the local Nu_t increases with the increase of τ. From the deviation of curves, it is also found that for a system with a larger τ, the radiation has a stronger effect on Nu_t. Therefore, it is concluded that more heat is transferred from a medium with a higher τ than that with a lower τ.

Fig. 8 presents the effects of wall emissivity ε_w on the local fRe and Nu_t . Similarly, it is found in Fig. 8a that the effects of ε_w on the fRe are restricted in the downstream region. It is also observed that the stronger radiation effect, the less the value of fRe at the downstream. Apparently, the local Nu_t with radiation effect is larger than that without radiation effect. In addition, Nu_t increases as the wall emissivity ε_w increases. The heat transfer is the maximum for a black duct ($\varepsilon_w = 1$).

In many applications, scattering processes are important in radiative heat transfer if particulates are present in the fluid. Therefore, the effects of the single scattering albedo on the fluid flow and heat transfer are of interest. For illustration, the scattering is assumed to be isotropic. Fig. 9 presents the effects of single scattering albedo ω on the axial variations of local fRe and Nu_t. The amount of energy that impinges upon the gray medium depends on the scattering albedo. When single scattering albedo ω approaches zero, the emission and absorption of the radiative energy within the medium dominate. But as the scattering albedo ω approaches unity, the scattering of the radiative heat transfer dominates. Hence, it is obvious in Fig. 9 that when ω is 0, the local fRe is attenuated significantly due to the most radiation effects. In addition, the local Nu_t decreases with increasing ω.

5. Conclusions

The characteristics of mixed convective flow and heat transfer in horizontal duct with radiation effects have been numerically studied. The effects of Rayleigh number, aspect ratio γ of the duct, conduction-to-radiation parameter N_c, optical thickness, wall emissivity, and single scattering albedo on momentum, heat and mass transfer have been analyzed in detail. Brief summaries of the major results are listed in the following:

1. For the same buoyancy situation, the flow with radiation shows a more rapid thermal development than the flow without radiation, and the local total Nusselt number is augmented by the radiation effect.

2. Results show that fRe and Nu_t increases as γ decreases for larger Ra. Also, fRe and Nu_t at the downstream are the least for $\gamma = 1$ among the three studied cases.
3. Buoyancy shows much stronger effect on the local friction factor than other parameters mentioned in the research. Both the local friction factor and total Nusselt number are increased by buoyancy.
4. The local total Nusselt number is increased by increasing optical thickness of the gray medium, wall emissivity and reducing single scattering albedo.

Acknowledgements

The authors would like to acknowledge the financial support of the present work by the National Science Council, R.O.C. through the contract NSC93-2212-E211-011. The financial support from Northern Taiwan Institute of Science and Technology is also acknowledged.

References

[1] F.P. Incropera, J.A. Schutt, Numerical simulation of laminar mixed convection in the entrance region of horizontal rectangular ducts, Numer. Heat Transfer 8 (1985) 707–729.
[2] H.V. Mahaney, F.P. Incropera, S. Ramadhyani, Development of laminar mixed convection flow in a horizontal rectangular duct with uniform bottom heating, Numer. Heat Transfer 12 (1987) 137–155.
[3] M. Wang, T. Tsuji, Y. Nagano, Mixed convection with flow reversal in the thermal entrance region of horizontal and vertical pipes, Int. J. Heat Mass Transfer 37 (1994) 2305–2319.
[4] W.M. Yan, Turbulent mixed convection heat and mass transfer in a wetted channel, ASME J. Heat Transfer 117 (1995) 229–233.
[5] Z.A. Hammou, B. Benhamou, N. Galanis, J. Orfi, Laminar mixed convection of humid air in a vertical channel with evaporation or condensation at the wall, Int. J. Therm. Sci. 43 (2004) 531–539.
[6] C.C. Huang, W.M. Yan, J.H. Jang, Laminar mixed convection heat and mass transfer in a vertical rectangular duct with film evaporation and condensation, Int. J. Heat Mass Transfer 48 (2005) 1772–1784.
[7] J.H. Jang, W.M. Yan, C.C. Huang, Mixed convection heat transfer enhancement through film evaporation in inclined square ducts, Int. J. Heat Mass Transfer 48 (2005) 2117–2125.
[8] F.C. Chou, G.J. Hwang, Vorticity–velocity method for the Graetz problem and the effect of natural convection in a horizontal rectangular channel with uniform wall heat flux, ASME J. Heat Transfer 109 (1987) 704–710.
[9] K.C. Cheng, S.W. Hong, G.J. Hwang, Buoyancy effects on laminar heat transfer in the thermal entrance region of horizontal rectangular channels with uniform wall heat flux for large Prandtl number fluid, Int. J. Heat Mass Transfer 15 (1972) 1819–1836.
[10] J.W. Ou, K.C. Cheng, R.C. Lin, Natural convection effects on Graetz problem in horizontal rectangular channels with uniform wall temperature for large Pr, Int. J. Heat Mass Transfer 17 (1974) 835–843.
[11] K.C. Cheng, J.W. Ou, Convection instability and finite amplitude convection in the entrance region of horizontal rectangular channels heated from below, in: Proceedings of 7th International Heat Transfer Conference, vol. 2, 1982, pp. 189–194.
[12] C.A. Hieber, S.K. Sreenivasan, Mixed convection in an isothermally heated horizontal pipe, Int. J. Heat Mass Transfer 17 (1974) 1337–1348.
[13] S.W. Hong, S.M. Morcos, A.E. Bergles, Analysis and experimental results for combined forced and free laminar convection in horizontal tubes, in: Proceedings of the 5th International Heat Transfer Conference, vol. 3, 1974, pp. 154–158.
[14] J.W. Ou, K.C. Cheng, Natural convection effects on Graetz problem in horizontal isothermal tubes, Int. J. Heat Mass Transfer 20 (1977) 953–960.
[15] M. Hishida, Y. Nagano, M.S. Montesclaros, Combined forced and free convection in the entrance region of an isothermally heated horizontal pipe, J. Heat Transfer 104 (1982) 153–159.
[16] R. Echigo, S. Hasegawa, K. Kamiuto, Composite heat transfer in a pipe with thermal radiation of two-dimensional propagation in connection with the temperature rise in a flowing medium upstream of a heating section, Int. J. Heat Mass Transfer 18 (1975) 1149–1159.
[17] A.T. Wassel, D.K. Edwards, Molecular radiation in a laminar or turbulent pipe flow, ASME J. Heat Transfer 98 (1976) 01–107.
[18] F.H. Azad, M.F. Modest, Combined radiation and convection in absorbing emitting and anisotropically scattering gas-particulate tube flow, Int. J. Heat Mass Transfer 24 (1981) 1681–1697.
[19] T. Seo, D.A. Kaminski, M.K. Jensen, Combined convection and radiation in simultaneously developing flow and heat transfer with nongray gas mixtures, Numer. Heat Transfer Part A 26 (1994) 49–66.
[20] L.K. Yang, Combined mixed convection and radiation in a vertical pipe, Int. Commun. Heat Mass Transfer 18 (1991) 419–430.
[21] L.K. Yang, Forced convection in a vertical pipe with combined buoyancy and radiation effects, Int. Commun. Heat Mass Transfer 19 (1992) 249–262.
[22] W.M. Yan, H.Y. Li, D. Lin, Mixed convection heat transfer in a radially rotating square duct with radiation effects, Int. J. Heat Mass Transfer 42 (1999) 35–47.
[23] W.M. Yan, H.Y. Li, Radiation effects on mixed convection heat transfer in a vertical square duct, Int. J. Heat Mass Transfer 44 (2001) 1401–1410.
[24] C. Debbissi, J. Orfi, S. Ben Nasrallah, Evaporation of water by free convection in a vertical channel including effects of wall radiative properties, Int. J. Heat Mass Transfer 44 (2001) 811–826.
[25] A.Y. Bakier, R.S.R. Gorla, Thermal radiation effect on mixed convection from horizontal surfaces in saturated porous media, Transp. Porous Media 23 (1996) 357–363.
[26] A.Y. Bakier, Thermal radiation effect on mixed convection from vertical surfaces in saturated porous media, Int. Commun. Heat Mass Transfer 28 (2001) 119–126.
[27] Y.J. Kim, A.G. Fedorov, Transient mixed radiative convection flow of a micropolar fluid past a moving, semi-infinite vertical porous plate, Int. J. Heat Mass Transfer 46 (2003) 1751–1758.
[28] E. Sediki, A. Soufiani, M.S. Sifaoui, Combined gas radiation and laminar mixed convection in vertical circular tubes, Int. J. Heat Fluid flow 24 (2003) 736–743.
[29] K. Ramakrishna, S.G. Rubin, P.K. Khosla, Laminar natural convection along vertical square ducts, Numer. Heat Transfer 5 (1982) 59–79.
[30] P.J. Roche, Computational Fluid Dynamics, Reinhold, New York, 1971, pp. 61–64.
[31] W.M. Yan, C.Y. Soong, Simultaneously developing mixed convection in radially rotating rectangular ducts, Int. J. Heat Mass Transfer 38 (1995) 665–677.
[32] W.A. Fiveland, Three-dimensional radiative heat transfer solution by the discrete-ordinates method, J. Thermophys. Heat Transfer 2 (1988) 309–316.
[33] T.Y. Kim, S.W. Baek, Analysis of combined conductive and radiative heat transfer in a two-dimensional rectangular enclosure using the discrete ordinates method, Int. J. Heat Mass Transfer 34 (1991) 2265–2273.
[34] M.F. Modest, Radiative Heat Transfer, McGraw-Hill, New York, 1993, pp. 541–571.
[35] B.G. Carlson, K.D. Lathrop, Transport theory: the method of discrete ordinates, in: H. Greenspan, C.N. Kelber, D. Okrent (Eds.), Computing Methods in Reactor Physics, Gordon & Breach, New York, 1968, pp. 165–266.